International Journal of Computing and Digital Systems
ISSN (2210-142X)
Int. J. Com. Dig. Sys. 12, No.1 (Oct-2022)

https://dx.doi.org/10.12785/ijcds/120191

# Stochastic Modeling of Interference in 5G mmWave Cellular Networks

**Yusra Banday[1], Gh. Rasool Begh[2] and Ghulam Mohammad Rather[3]**

[1,2,3]*Department of Electronics and Communication Engineering, Advance Communication Lab, National Institute of Technology, Hazratbal, Srinagar 190006, India*

*Received 22 Jan. 2021, Revised 15 Jul. 2022, Accepted 23 Jul. 2022, Published 31 Oct. 2022*

**Abstract:** A simpler statistical interference model for millimeter-wave (mmWave) cellular networks for use in 5G is proposed in this work. The accuracy of this model is examined in an outdoor cellular network with different scenarios. The interference accuracy coefficient (IAC) is introduced to quantify the accuracy of predicting an outage event and the similarity between various interference models. In this paper, different signal-to-interference-plus-noise-ratio (SINR) distributions are used and a new framework has been proposed to quantify the similarity between SINR distributions of existing interference models. It is observed that the accuracy of millimeter-wave cellular networks is modeled by simpler interference models which are less erroneous compared to the models used for performance analysis in microwave networks. The results obtained in this work clearly show that in the mmWave networks scenarios with obstacles, the simple interference models are accurate enough. However, in omnidirectional communications, the interference models required are quite complex. Furthermore, in this work, the interference in mmWave networks with a deterministic channel is also modeled using the proposed Two-Ball interference model. This model gives the appropriate results of blockage events due to outages in mmWave networks.

**Keywords:** SINR, mmWave, Interference, 5G

## 1. Introduction

The unprecedented demand of traffic by users motivates the wireless service providers to leverage the extremely high frequency or mmWave band frequencies. The usage of mmWave ultrawideband networks with larger band breadth, enables ultra-low latency, high data rate, massive connectivity, and low battery consumption in 5G cellular networks[1]. From the numerical and analytical results obtained in this paper, it is evident that the narrow beams radiated from antennas at mmWave frequencies are highly sensitive to the density of obstacles present in the network environment [2]. The varying density of obstacles significantly affects the signal attenuation and therefore the distribution of SINR.

Interference management in 5G networks is a complex process because a large number of small and heterogeneous devices are interconnected. These are referred to as heterogeneous networks or HetNets. This type of architecture gives rise to multiple tiers of different sizes and transmission powers. Therefore simple modeling of interference in 5G mmWave networks is a major concern.

One of the distinguishing characteristics of mmWave communications is blockage or high penetration loss. To determine the outage probability due to blockage, SINR is used as an evaluation metric. The human body accounts for a penetration loss of 20-35 dB in mmWave communication [3]. From the mathematical expression of SINR, it depends on multiple parameters like antenna patterns, channel estimation errors, first-order reflection in millimeter-wave networks, receiver design, and transmission power [4], [5]. This makes it challenging to accurately design the 5G mmWave networks on basis of SINR. This results in the motivation for the development of simpler interference models to address these issues through mathematical modeling. Furthermore, for mathematical analysis, the proposed interference models should be tractable. These interference models for 5G millimeter-wave networks should be accurate and adequate to simplify the design parameters in a particular network setting. In this work, a statistical approach is used to model interference in 5G mmWave networks. Furthermore, a parameter called an Interference Accuracy Coefficient [IAC] has been introduced to quantify the similarity between various interference models. In the proposed model a typical outdoor cellular network is taken

*E-mail address: yusra_01phd16@nitsri.ac.in*

into account.

The works carried out earlier to study the interference modeling in the mmWave frequency band take into consideration the single link communication system[6]. Therefore, the realistic measurements in operational 5G cellular networks are lacking in the literature. To bridge this divide, we have carried out the calculations at commercial frequency ranges of 5G at sub-6 GHz and 28 GHz frequencies. This can help in the extension of this work to explore and develop various interference models in different environmental scenarios.

Various existing mathematical approaches like Bhattacharya distance, Kullback-Leibler, and Hallinger distance are used to measure the similarity between any two distributions. From the calculations summarized in Table I and Table II, it is clear that the distance between the probability distributions is evaluated and mapped in entire support to only one real value. In such cases, the results can be misleading because possibly the two distributions can be very close or similar in certain required ranges of SINR. Beyond these ranges, the values of SINR can diverge. These existing distance measures used in our work compare two distributions over the entire range, this results in large dissimilarity or distance between two distributions and leads to mistakenly avoiding the use of a simplified interference model. However, IAC compares the distance between two distributions only at a specific threshold which gives more accurate results.

In this work, a new proposed framework is used to quantify the similarity between SINR distributions of existing interference models. The comparison of the existing and the proposed method shows the performance improvement offered by the proposed technique. Hence this work complements the existing techniques present in the literature on interference management.

In this paper, various methods are used to compute and model the distribution of SINR. These interference models consider many trade-offs between accuracy and complexity. IAC is implemented in the microwave and mmWave scenarios with a simulation of a Poisson network using Monte Carlo simulation (MCM). A simpler interference model for mmWave networks is developed with natural assumptions like negligible side-lobes and infinite penetration loss. The accuracy of interference models is then mathematically evaluated in both of these network settings. The results are simulated and plotted for further evaluation. The parameters used for evaluation are miss-detection and false-alarm explained in detail in the following sections. Depending on the modeling of multiple interferers, MAC protocols, antenna patterns, design of receiver, complexity, and network topology, an interference model can be designed [5].

The rest of the paper is organized as follows. In Section 2 mathematical analysis of existing distance measures is carried and results are compared to the proposed method. An exhaustive literature survey of various interference models that can be used in mmWave networks is carried out. Based on this survey, a statistical interference model is proposed that can correctly predict outage events and model an interference in 5G networks. In section 3, system models are illustrated and numerically evaluated for various network scenarios. The accuracy of the proposed model is quantified using IAC. This coefficient is compared with the previously used similarity indices like the Bhattacharya coefficient (BC) and Kullback-Liebler (KL) Divergence. A detailed description of the proposed statistical mmWave interference model is also given in section 4. The results of this model are validated for different network scenarios, propagation channels, carrier frequencies, and densities of Base Stations and user equipment. The paper is concluded in Section 5.

## 2. Related Work

In this section, various interference models are discussed. These models consider the impact of those interferers in a network that contributes to the maximum interference. As more interferers are taken into consideration, the accuracy of a model increases but this increases complexity as well [7]. Given this, the Primary Interference Model (PIM) is considered to be the simplest one. In this model, an outage is said to occur when two communication links end at the same point. This creates self-interference and necessitates the use of a half-duplex mode of communication. To improve the accuracy of PIM, Interference Range Model (IRM) is used [8]. Here an outage event occurs if the closest interferer is located within an interference range. To estimate the outage probability in a network, the SINR metric is used. For the mathematical analysis and simulations, consider a communication link having a pair of transmitter and an intended receiver. Let S be the power from the intended transmitter, $\eta$ be the white Gaussian noise power, ik be the interference from interferer $k \in \mathfrak{T}$ where $\mathfrak{T}$ is the set of interferers which consist of all the active transmitters except the intended one. Thus the SINR at the reference receiver is given by

$$\gamma_i = \frac{S}{\sum\limits_{k\in\mathfrak{T}} i_k + \eta} \tag{1}$$

This equation can be re-written as

$$\gamma = \frac{P_i g_i^{Tx} g_i^{Rx} g_i^{Ch}}{\sum\limits_{k\in\mathfrak{T}} p_k g_k^{Tx} g_k^{Rx} g_k^{Ch} + \eta} \tag{2}$$

where
$P_i$ =Power transmitted by a transmitter
$g_i^{Ch}$ = Channel gain between intended transmitter $TX_i$ and reference receiver
$g_i^{Tx}$ = Antenna gain at $TX_i$ towards the reference receiver
$g_i^{Rx}$ = Antenna gain at reference receiver towards $TX_i$
$\eta$ = white Gaussian noise power

If $\beta$ represents the SINR threshold then an outage is said to occur if the total SINR at the intended receiver is less than the threshold i.e. $\gamma < \beta$. This probability of an outage is given by a statistical model of interference known as statistical distribution describing [9]. In mmWave networks, modeling of the statistical distribution describing is difficult due to the presence of various probability distributions of random variables in the numerator and denominator of Equation (2). More elements of randomness are contributed due to high penetration losses, antenna pattern, and first-order reflection in mmWave networks [5].

The interference range is defined as the distance of the closest interferer from the receiver. If this distance is set to zero, IRM tends to PIM. With modification in the interference range of IRM a new model called the Protocol Model (PRM) has been proposed in [10]. In the IRM model, the interference range is a constant quantity whereas in PRM case it is a variable depending on:

1) The value of the SINR threshold at which the signal can be successfully decoded.
2) Power received from the intended transmitter.

An interference range in PRM is defined as $r_{PRM} = (1 + \Delta)d_0$, where $\Delta$ is a positive real constant [10] and $d_0$ is the distance between nodes in a cell. In PRM an outage event takes place if all the active transmitters are within an interference range of $r_{PRM}$ [10]. These above-mentioned models are simpler but offer less accuracy because there is a probability of having an active transmitter (interferer) beyond the interference range. This results in the fade of signal strength and hence the value of SINR falls below the assumed threshold value. IRM and PRM do not account for the interference caused by an active transmitter located beyond the predefined interference range. Moreover,these models are used at network layer for performance analysis and system design to model throughput [11], [12], [13], topology control [14], [15], routing [16], delay[17], [18] and backoff design [19].

To overcome issues of IRM and PRM, the Interference Ball Model (IBM) [20] is used. This model takes into account the effect of all the near-field interferers that are located within a certain distance. This is achieved at the cost of higher complexity of IBM as compared to PRM and IRM. The outage event in IBM occurs if total SINR due to transmitters with interference range rIBM falls below threshold signal level $\beta$[21]. In wireless networks, IBM is used for performance analysis [21], [22], [23], [24].

If there is a set of transmitters and receivers, we define strong links as having an individual channel gain greater than a certain predefined threshold [25]. With this assumption Topological Interference Model (TIM) is defined. This model is used for the degree of freedom analysis and capacity evaluation [25], [26]. The outage occurs at any receiver i when SINR due to all transmitters having strong links is less than $\beta$ [25].

At the physical layer, Physical Model (PhyM/SINR) interference model is used. This model takes into account all the active transmitters (interferers) present in a network. An outage is said to occur if the value of SINR due to all the transmitters drops below the threshold $\beta$ [10].

To provide a uniform overview of the effect of all interference models in different network scenarios, some random variables are defined on a link between a transmitter and receiver for each model. These random variables like $\alpha_k^X$ are associated with links between transmitter $k$ which belongs to a set of interferers $\mathfrak{T}$ i.e. $k \in \mathfrak{T}$ and a typical receiver $i$.

1) For PRM; $\alpha_k^{PRM}$ is defined as:
$$\alpha_k^{PRM} = \begin{cases} +\infty, & d_k \leq (1+\Delta)d_0 \\ 0, & \text{otherwise} \end{cases}$$
2) For IBM; $\alpha_k^{IBM}$ is defined as:
$$\alpha_k^{IBM} = \begin{cases} 1, & d_k \leq r_{IBM} \\ 0, & \text{otherwise} \end{cases}$$
$d_k \leq r_{IBM}$ indicates that all transmitters are within interference range
3) For TIM; $\alpha_k^{TIM}$
$$\alpha_k^{TIM} = \begin{cases} 1, & g_k^{ch} > \varepsilon_o \\ 0, & \text{otherwise} \end{cases}$$
4) For PhyM;
$\alpha_k^{PhyM} \triangleq 1$ for $k \in \mathfrak{T}$

A virtual channel gain for the interference models is defined as $g_k^X = \alpha_k^x g_k^{ch}$ where x denotes PhyM, IBM, TIM, and PRM, $g_k^{ch}$ is a channel gain, $\alpha_k^X$ is a random variable used to model the channel gain in these different interference models.

In the existing literature, the following metrics for computing similarity between distributions are used:

1) Bhattacharyya Distance
2) Kullback Leibler Divergence
3) Hellinger Divergence

In this paper, the parameter IAC is introduced for evaluating the similarity between probability distributions.

### A. *Definition of Interference Accuracy Coefficient (IAC)*

A wireless network is taken into consideration. Let an interference model Z represent this network. SINR of a reference receiver in this network model can be represented by $\Upsilon^z$. For this model, a binary hypothesis test is carried out. The two values which denote the absence and presence of an outage event are $H_0$ and $H_1$ respectively.

$$\begin{cases} H_0 : \Upsilon^z \geq \beta & \text{Absence of an outage event} \\ H_0 : \Upsilon^z < \beta & \text{Presence of an outage event} \end{cases}$$

Consider another test interference model y defined under any set of functions that describe a wireless network. The

difference in the functions/parameters of these two models is reflected in the overall deviation of the individual SINR of the models. This deviation is quantified by Interference Accuracy Coefficient (IAC).

In this manner, the characterization of the accuracy of performance analysis using model $y$ instead of $z$ is done. Taking the outage parameter into account, models $y$ and $z$ are said to be similar if their results of outage events are the same.

Assume that a test interference model y detects all the outage events of reference model $z$. Then the performance of $y$ can be evaluated by computing false-alarm and miss-detection.

### B. Definition of false-alarm

False alarm represents an outage event under hypothesis Ho. Test model y predicts an outage i.e. $\Upsilon^y < \beta$ under the condition that reference interference model $z$ declares no interference i.e. $\Upsilon^z \geq \beta$. Hence the probability of false-alarm of any interference model $y$ can be represented as:

$$p_{fa}^{y/z} = p_r\{\Upsilon^y < \beta | \Upsilon^z \geq \beta\}$$

$$p_{fa}^{y/z} = \frac{[p_r(\Upsilon^y < \beta) \cap (\Upsilon^z \geq \beta)]}{p_r[(\Upsilon^z \geq \beta\})]}$$

### C. Definition of miss-detection

Miss detection represents an outage event under hypothesis $H_1$. Test model $y$ fails to detect an outage event i.e. $\Upsilon^y\beta$. While hypothesis H1 signifies the occurrence of an outage i.e.$\Upsilon^z < \beta$. Therefore, the probability of miss-detection

$$p_{md}^{y/z} = p_r\{\Upsilon^y \geq \beta | \Upsilon^z < \beta\}$$

$$p_{md}^{y/z} = \frac{[p_r(\Upsilon^y \geq \beta) \cap (\Upsilon^z < \beta)]}{p_r[(\Upsilon^z < \beta\})]}$$

These probabilities $p_{fa}^{y/z}$ and $p_{md}^{y/z}$ quantify the similarity in the detection of outage events by interference models $y$ and $z$.

IAC is used to quantify the similarity of interference models at the SINR threshold $\beta$ by using the notions of false-alarm and miss-detection. For any constant $0 \leq \xi \leq 1$ and SINR threshold $\beta$, similarity $S$ of interference model $y$ to $z$ can be defined as:

$$\begin{aligned} S_{\xi,\beta}(y||z) &= \xi(1 - p_{fa}^{y/z}) + (1 - xi)\left(1 - p_{md}^{y/z}\right) \\ &= 1 - \xi p_{fa}^{y/z} - p_{md}^{y/z}(1 - \xi) \end{aligned} \tag{3}$$

Since $S_{\xi,\beta}(y||z)$ is purely dependent on probabilities, it ranges from 0 to 1.0 represents no similarity and 1 denotes that model $y$ is similar to $z$ in capturing outage.

#### 1) Validation of IAC

In terms of density functions, IAC measures the distance of probability Density Function (PDF) of $\Upsilon^y$ from $\Upsilon^z$. The existing methods like Bhattacharyya Distance, Kullback Leibler Divergence, and Hellinger Distance can be misleading in most cases. Within a certain specific range of SINR values, two probability distributions can be very similar but beyond that range, they can deviate. Therefore, for that specific range, test interference model $y$ can be used. If the same distributions are evaluated for similarity using classical distance measuring methods they consider an entire range of values for comparison. These distributions can have higher distances or dissimilarities when compared over the whole range. Hence IAC is used to investigate if $f_{\Upsilon^y}$ is similar to $f_{\Upsilon^z}$ at any specific SINR threshold.

For validation of IAC, three discrete random variables $X, Y$, and $Z$ with the ranges $R_X = \{x_1, x_2, x_3\}$, $R_Y = \{y_1, y_2, y_3\}$ and $R_Z = \{z_1, z_2, z_3\}$ have been considered.

The respective probability mass functions are given in Table I. The metrics obtained from the above table are

TABLE I. Probability mass functions

| Sample Value | 1 | 2 | 3 |
|---|---|---|---|
| $f_X(x)$ | 0.07 | 0.4 | 0.53 |
| $f_Y(y)$ | 0.2 | 0.4 | 0.4 |
| $f_Z(z)$ | 0.25 | 0.3 | 0.45 |

$f_X, f_Y$, and $f_X, f_Z$ taking $f_X$ as reference.

*Kullback-Leibler Divergence* is also called relative entropy. It gives a measure of divergence of one probability distribution from a reference distribution. Two distributions are said to be identical if KL=0 [27].

Mathematically KL divergence is represented by

$$D_{KL} = (Q||P) = \sum_i Q(i) \ln\left[\frac{Q(i)}{P(i)}\right]$$

where $P(i)$ and $Q(i)$ are two discrete probability distributions [27].

$D_{KL}(f_x||f_y) = 0.2 \log\left(\frac{0.2}{0.07}\right) + 0.4 \log\left(\frac{0.4}{0.4}\right) + 0.4\left(\log \frac{0.4}{0.53}\right)$

$D_{KL}(f_x||f_y) = 0.0423$

$D_{KL}(f_x||f_z) = 0.25 \log\left(\frac{0.25}{0.07}\right) + 0.3 \log\left(\frac{0.3}{0.4}\right) + 0.45 \log\left(\frac{0.45}{0.53}\right)$

$D_{KL}(f_x||f_z) = 0.06875$

*Bhattacharyya Distance* is used to measure the similarity of two probability distributions over the same domain $X$. If $P$ and $Q$ are any two distributions then Bhattacharyya distance $DB(p, q) = -\ln[BC(p, q)]$.

$BC$ is a Bhattacharyya coefficient represented mathematically by

$$BC(p, q) = \sum_{x \in X} \sqrt{p(x)q(x)}$$

The smaller the values of DB, the higher is the similarity. If DB=0, two distributions are identical.

Bhattacharyya coefficient is used for discrete probability distributions.

$0 \leq BC \leq 1$

$0 \leq D_B \leq \infty$

$D_B$ for Table 1 can be calculated by

$$\begin{aligned} BC(f_x, f_y) &= \sqrt{0.07 \times 0.2} + \sqrt{0.4 \times 0.4} + \sqrt{0.53 \times 0.4} \\ &= 0.9787 \\ DB &= \ln[BC(f_x, f_y)] \\ DB &= 0.02147 \\ BC(f_x, f_z) &= \sqrt{0.07 \times 0.25} + \sqrt{0.3 \times 0.4} + \sqrt{0.45 \times 0.53} \\ &= 0.9670 \\ DB &= 0.03349 \end{aligned}$$

*Euclidean Distance* measures the difference between two probability distributions. The distance between two distributions $f_x, f_y$ is given by

$$\begin{aligned} d(f_x, f_y) &= \sqrt{(0.2-0.07)^2 + (0.4-0.4)^2 + (0.4-0.53)^2} \\ &= 0.18384 \\ d(f_x, f_z) &= \sqrt{(0.25-0.07)^2 + (0.3-0.4)^2 + (0.45-0.53)^2} \\ &= 0.2209 \end{aligned}$$

*Hellinger distance* quantifies the similarity between two probability distributions $P$ and $Q$.
Mathematically Hellinger distance $H(P, Q)$ is given by

$$H(P,Q) = \frac{1}{\sqrt{2}} \sqrt{\sum_{i=k}^{k} \left(\sqrt{p_i} - \sqrt{q_i}\right)^2}$$

$$H(x,y) = \frac{1}{\sqrt{2}} \sqrt{\begin{array}{l} \left(\sqrt{0.07} - \sqrt{0.2}\right)^2 + \left(\sqrt{0.4} - \sqrt{0.4}\right)^2 \\ + \left(\sqrt{0.53} - \sqrt{0.4}\right)^2 \end{array}}$$

$H(x, y) = 0.1457$
Similarly, $H(x, z) = 0.18148$ From Table I and Table II, it

TABLE II. Existing distance measures

| Distributions | $f_x, f_y$ | $f_x, f_z$ |
|---|---|---|
| Kullback-Liebler (KL) | 0.0423 | 0.06875 |
| Bhattacharyya Distance | 0.02147 | 0.03349 |
| Euclidean Distance | 0.18384 | 0.2209 |
| Hellinger Distance | 0.1457 | 0.18148 |

is evident that the existing measures evaluate the distance between two probability distributions in support of one real value only.

To extend the application of IAC in investigating the accuracy of interference models, we consider different network scenarios. For the same network setting KL divergence and Bhattacharyya distance is computed and compared, corresponding to different Interference accuracy coefficient values.

## 3. System Model

To validate the proposed interference model, we consider an existing omnidirectional communication with rayleigh fading and evaluate this scenario for various interference models. The simulations are carried out in MATLAB and results obtained are compared with the deterministic channel and directional communication in 5G mmWave networks for the parameters like blockage and directionality.

**Scenario-I:** Evaluation of the accuracy of reference interference models with respect to the test model.

**Type of communication:** Omnidirectional
**Type of channel:** Rayleigh Fading

Let PhyM be a reference interference model $z$. Accuracy of test models $y$ viz; IBM, PRM, and TIM can be evaluated in the same network setting.

Consider a polar coordinate with a reference receiver at an origin. Let its intended transmitter be placed at a spatial length of $d_0$. A random number of interferers that are basically the unintended transmitters are modeled by homogenous Poisson distribution as shown in Figure 1.

Assumptions

1) $\lambda_t$ be the density of interferers on the plane.
2) All the transmitters are active and $P$ be the transmission power of each transmitter.
3) Interference cancellation is not employed.
4) In omnidirectional communication, antenna gain is unity $\therefore g_k^{Tx} = g_k^{Rx} = 1$ where $k \in \mathfrak{T}$

A geometrical annulus sector is defined as $A(\theta, r_{in}, r_{out})$. $\theta$ is an angle subtended by sector at a reference receiver located at the origin of a polar coordinate system. $r_{in}$ and $r_{out}$ are inner and outer radii respectively.

*Modeling of a communication channel*

1) Attenuation at a reference distance of 1m is considered to be constant and is denoted by $c$.
2) Rayleigh's fading coefficient is represented by $h$.
3) Let $\alpha$ be the attenuation which varies exponentially with distance.
4) At the origin of the polar coordinate system, power received by the reference receiver follows power-law; i.e. the signal attenuates as distance increases. To nullify the singularity at origin the path loss index is modeled by an indicator function.
   Indicator function of a subset $\overline{A}$ of a set $(2\pi, 0, a)$ maps elements of $(2\pi, 0, a)$ from {0,1}. $\theta$ takes the value of $\{0 - 2\pi\}$ over the whole cellular area. At origin $r_{in} = 0$ and $r_{out} = a$. Hence path loss is represented as $\alpha 1_{\overline{A}(2\pi,0,a)}$ . Here $1\{\cdot\}$ is an indicator function. This signifies that the transmitters located inside the disk will undergo no attenuation.
5) The signal from transmitters located outside the disk at a radius of '$a$' will undergo attenuation according to a power law.

Thus the channel gain of a link between the intended transmitter and reference receiver at a distance of $d_i$ is given by

$$g_i^{ch} = c \times h_i \times d_i^{-\alpha 1_{\overline{A}(2\pi,0,a)}} \tag{4}$$

*Analysis of Accuracy of IBM*

$$\gamma^{IBM} = \frac{P_0 g_0^{Tx} g_0^{Rx} g_0^{ch}}{\sum\limits_{k \in \mathfrak{T}} p_k g_k^{Tx} g_k^{Rx} g_k^{ch} + \eta} \tag{5}$$

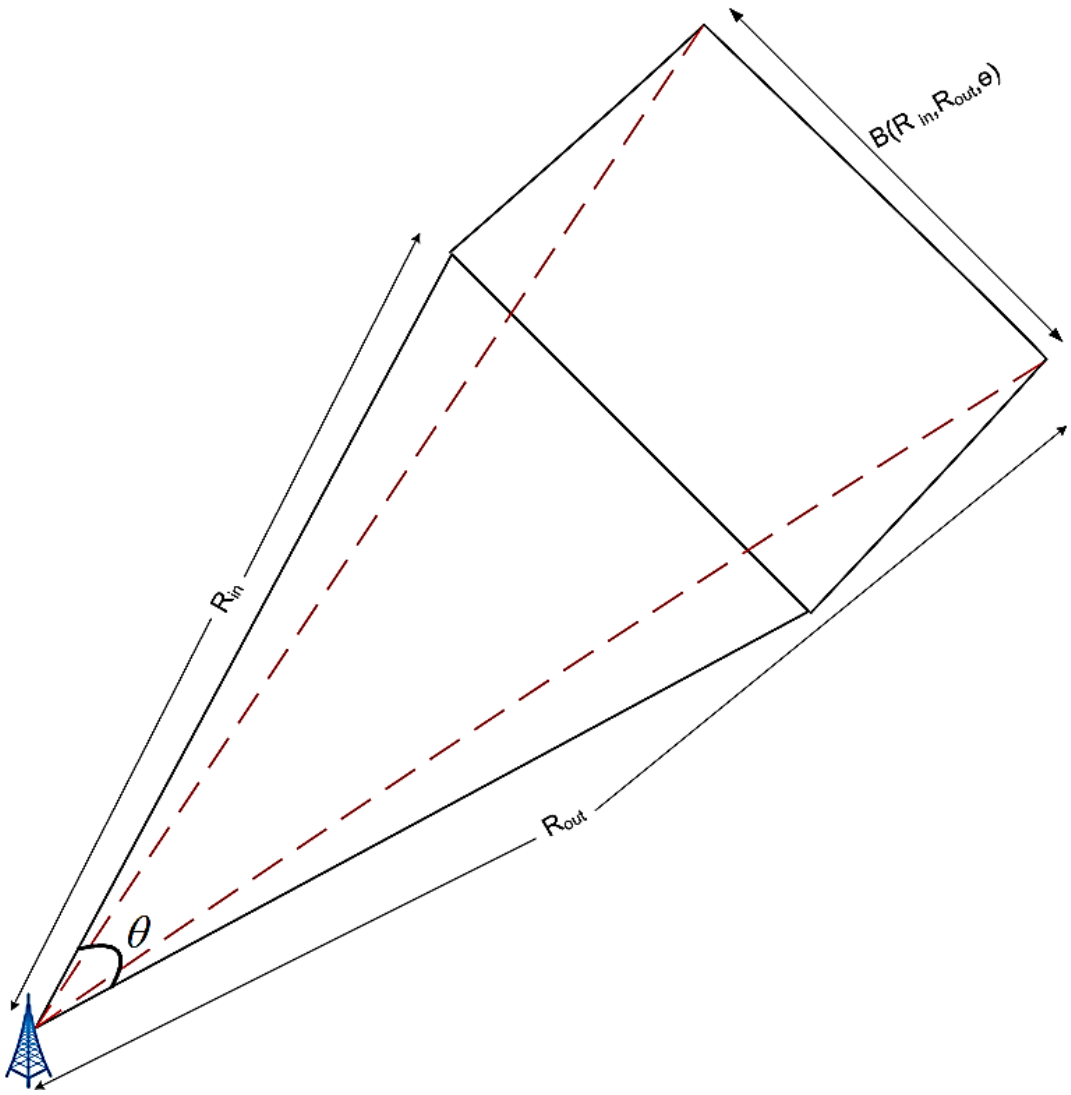


Figure 1. Spatial distribution of interferers

For the omnidirectional radiation pattern of antenna $g_0^{Tx} = g_0^{Rx} = 1$ and $g_k^{Tx} = g_k^{Tx} = 1$.

$$\gamma^{IBM} = \frac{P \times g_0^{ch}}{\sum\limits_{k \in \mathfrak{T} \cap A(2\pi,o,\gamma_{IBM})} p \times g_k^{ch} + \eta}$$

The lower bound in the first term of the denominator is used because in IBM interference is contributed mainly by near-field interferers in the interference range. Hence to simplify the mathematical analysis it is assumed that $\gamma_{IBM} \geq a$.

From Equations (2) and (4), and after some simplification, we obtain

$$\gamma^{IBM} = \frac{p \times c \times h_0 \times d_0^{-\alpha}}{\sum\limits_{k \in \mathfrak{T} \cap A(2\pi,o,\gamma_{IBM})} p \times c \times h_k \times d_k^{-\alpha 1_{\bar{A}(2\pi,0,a)}} + \eta} \quad (6)$$

$$\gamma^{IBM} = \frac{h_0 \times d_0^{-\alpha}}{\sum\limits_{k \in \mathfrak{T} \cap A(2\pi,0,\gamma_{IBM})} h_k \times d_k^{-\alpha 1_{\bar{A}(2\pi,0,a)}} + \eta/p \times c}$$

In Appendix A, we have derived

$$p_r\left[\gamma^{IBM} < \beta\right] = 1 - p_r\left[h_0 \geq \left(\sum_{k \in \mathfrak{T} \cap A(2\pi,0,\gamma_{IBM})} h_k \times d_k^{-\alpha 1_{\bar{A}(2\pi,0,a)}} + \eta/p \times c\right)\beta d_0^{\alpha}\right]$$

The PDF of a Rayleigh distribution function is given by $\frac{r}{\sigma^2}\exp\left(\frac{-r^2}{2\sigma^2}\right)$[28]

$\therefore$ PDF of $h_0$ is given as $f_{h_0} = h_0 e^{-h_0 x}$[28]

If $h_0 = 1, f_{h_0} = e^{-x}$ (7)

$$\Rightarrow p_r\left[\gamma^{IBM}<\beta\right]=1-E_{I,h}\left[\left(\sum_{k\in\mathfrak{T}\cap A(2\pi,0,\gamma_{IBM})} h_k\times d_k^{-\alpha 1_{\overline{A}(2\pi,0,a)}} +\eta/p\times c\right)\beta d_0^{\alpha}\right]$$

Substituting the value of PDF term in summation in Appendix A, from Equation (7) we get

$$p_r\left[\gamma^{IBM}<\beta\right]=1-\exp\left(\frac{-\eta\beta d_0^{\alpha}}{p\times c}\right)E_I \left[\prod_{k\in\mathfrak{T}\cap A(2\pi,0,\gamma_{IBM})} E_h\left[\exp\left\{-\beta d_0^{\alpha}h_k d_k^{-\alpha 1_{\overline{A}(2\pi,0,a)}}\right\}\right)\right] \quad (8)$$

$h_1, h_2, h_3 \ldots\ldots h_k$ denotes the Rayleigh fading coefficient on each separate link $k$. $\mathfrak{T}$ denotes the whole set of a number of interferers. Therefore, $h$ and $\mathfrak{T}$ are independent variables whose expectation values can be separated.
From probability generating functional, for a stationary Poisson ($\lambda$) process[29].

$$G(\xi)=E\left\{\prod_i \xi(t_i)\right\}$$
$$G(\xi)=\exp\{-\lambda\int[1-\xi(t)dt\}$$

From the above two equations

$$\begin{aligned} G(\xi) &= \exp\left\{-2\pi\lambda_t\int_0^{\infty} 1_{A(2\pi,0,\gamma_{IBM}}(1- E_h\left[e^{-\beta d_0^{\alpha}hr^{-\alpha 1_{\overline{A}(2\pi,0,a)}}}\right])rdr\right\} \\ &= \exp\left\{-2\pi\lambda_t E_h\left[\int_0^{\infty} 1_{A(2\pi,0,\gamma_{IBM}}(1- e^{-\beta d_0^{\alpha}hr^{-\alpha 1_{\overline{A}(2\pi,0,a)}}}\right)rdr\right]\right\} \end{aligned}$$

Since within the range of 0–a, the indicator function $1_{\overline{A}(2\pi,0,a)}$ is zero.
$\therefore r^{-\alpha 1_{\overline{A}(2\pi,0,a)}}=r^0=1$

$$\Rightarrow G(\xi)=\exp\left\{-2\pi\lambda_t E_h\left[\int_0^a\left(1-e^{-\beta d_0^{\alpha}h}\right)rdr + \int_a^{r_{IBM}}\left(1-e^{-\beta d_0^{\alpha}hr^{-\alpha}}\right)rdr\right]\right\}$$

In Appendix B, Equation (9) is obtained as under:

$$p_r\left[\gamma^{IBM}<\beta\right]=1-\left\{\exp\left(\frac{-\eta\beta d_0^{\alpha}}{p\times c}\right)-2\pi\lambda_t E_h\left[\frac{a^2}{2}\left(1-e^{-\beta d_0^{\alpha}h}\right)+\left(\frac{r_{IBM}^2-a^2}{2}\right) -\left[\Gamma\left(\frac{2}{\alpha},\frac{\beta d_0^{\alpha}h}{r_{IBM}^{\alpha}}\right)-\Gamma\left(-\frac{2}{\alpha},\frac{\beta d_0^{\alpha}h}{a^{\alpha}}\right)\right]\frac{(\beta d_0^{\alpha}h)^{2/\alpha}}{\alpha}\right]\right\} \quad (9)$$

The probability of false alarm in IBM with respect to test model PhyM

$$P_{fa}^{IMB/PhyM}=P_r\left[\gamma^{IBM}<\beta/\gamma^{PhyM}\geq\beta\right] \quad (10)$$

From Bayes' theorem [29], as expressed in Appendix B, Equation (10) can be re-written as:

$$\begin{aligned} P_{fa}^{IBM/PhyM} &= \frac{P_r\left(\gamma^{IBM}<\beta\right)P_r\left(\gamma^{PhyM}\geq\beta/\gamma^{IBM}<\beta\right)}{P_r\left(\gamma^{PhyM}\geq\beta\right)} \\ P_{fa}^{IBM/PhyM} &= \frac{P_r\left(\gamma^{IBM}<\beta\right)P_r\left(\gamma^{PhyM}\geq\beta/\gamma^{IBM}<\beta\right)}{1-P_r\left(\gamma^{PhyM}<\beta\right)} \end{aligned} \quad (11)$$

In IBM interferers located in the near-field contribute to maximum interference while in PhyM, interference is due to interferers located over the entire network coverage area.

$$\gamma^{IBM}=\frac{\text{Signal Power}}{\text{Noise + Near Field Interference}} \quad (12)$$

$$\gamma^{PhyM}=\frac{\text{Signal Power}}{\text{Noise + Entire Network Interference}} \quad (13)$$

Comparing Equation (12) and Equation(13) it is clear that the second term of the denominator in Equation (12) will be lesser than in Equation (13).

Hence $\gamma^{IBM}>\gamma^{PhyM}$.

Thus the probability of $\gamma^{PhyM}>\beta$ given the condition $\gamma^{IBM}<\beta$ is zero.

$$\text{i.e., } P_r\left(\gamma^{PhyM}\geq\beta/\gamma^{IBM}<\beta\right) \quad (14)$$

$$\left[1-P_r\left(\gamma^{PhyM}<\beta/\gamma^{IBM}<\beta\right)\right]=0$$

$$\Rightarrow P_r\left(\gamma^{PhyM}<\beta/\gamma^{IBM}<\beta\right)=1 \quad (15)$$

Substitute Equation (14) in Equation (11), we get

$$P_{fa}^{IBM/PhyM}=0 \quad (16)$$

Thus we need to compute the miss-detection metric to estimate the total outage probability in a network.

$$\begin{aligned} P_{md}^{IBM/PhyM} &= P_r[\gamma^{IBM}\geq\beta/\gamma^{PhyM}<\beta] \\ &= 1-P_r[\gamma^{IBM}<\beta/\gamma^{PhyM}<\beta] \\ &= 1-\frac{P_r[\gamma^{IBM}<\beta]P_r[\gamma^{PhyM}<\beta/\gamma^{IBM}<\beta]}{P_r[\gamma^{PhyM}<\beta]} \end{aligned}$$

From Equation (15)

$$P_{md}^{IBM/PhyM}=1-\frac{P_r\left[\gamma^{IBM}<\beta\right]}{P_r\left[\gamma^{PhyM}<\beta\right]} \quad (17)$$

To obtain the value of $P_r\left[\gamma^{PhyM}<\beta\right]$, evaluate Equation (9) at $r_{IBM}\rightarrow\infty$ since PhyM considers interference over the whole network area.

$$P_r\left[\gamma^{PhyM}<\beta\right]=1-\left\{\exp\left(\frac{-\eta\beta d_0^{\alpha}}{p\times c}\right)-2\pi\lambda_t E_h\left[\frac{a^2}{2}\left(1-e^{-\beta d_0^{\alpha}h}\right)-\left(\frac{a^2}{2}\right)-\left[\Gamma\left(\frac{2}{\alpha}\right)-\Gamma\left(-\frac{2}{\alpha},\frac{\beta d_0^{\alpha}h}{a^{\alpha}}\right)\right]\frac{(\beta d_0^{\alpha}h)^{2/\alpha}}{\alpha}\right]\right\} \quad (18)$$

Substituting values from Equation (9) and from Equation (18) in Equation (17), the probability of miss-detection is calculated. Furthermore, from Equation(16), the probability of false-alarm for any SINR threshold $\beta$ is zero,i.e., $P_{fa}^{IBM/PhyM}=0$. As already discussed, from Equation (17), when $r_{IBM}\rightarrow\infty$, then probabilities of miss-detection of test interference model IBM and reference interference model PhyM follow an asymptotic distribution. Thus in such a scenario, from Equation (3), IAC $S_{(}\xi,\beta)(IBM\|PhyM)=1$. This indicates that two interference models are similar with the above conditions.

## 4. IMPLEMENTATION OF ACCURACY INDEX AT MICROWAVE AND MILLIMETER-WAVE FREQUENCIES

The accuracy of interference models is evaluated at sub-6 GHz and 28 GHz frequencies. An outdoor microwave network with Rayleigh fading channel as mentioned in [30] is considered. A Poisson network is simulated using a Monte Carlo simulation (MCM). $\lambda_t$ and $\lambda_0$ represent the density of interferers and obstacles respectively. dt denotes an average inter-transmitter distance. For ease of illustration, the notion $d_t = 1/\sqrt{\lambda_t}$ is used. This signifies the density of a cellular network.

If $d_t$ is small then the transmitters are closely spaced and provide high density to the network. Average inter-transmitter distance in a cellular network directly impacts the accuracy of its interference model. This also varies the probabilities $P_{md}$ and $P_{fa}$. In Figure 2, the accuracy of IBM is evaluated against inter-transmitter distance with various values of $r_{IBM}$. From Equation (17) when the interference range of IBM reaches infinity, $P_{md}^{IBM/PhyM}$ asymptotically tends to zero. Hence in combination with $P_{fa} = 0$, from Equation (3), $S_{(}\xi,\beta)(y||z) = 1$. This depicts the similarity of IBM and PhyM under no outage conditions.

This also shows that as rIBM increases, both probabilities of false-alarm and miss-detection tend to zero. Thus the accuracy of the interference model increases. With $r_{IBM} = 20$, and dense transmitter deployment, accuracy is maximum. As the inter-transmitter distance increases, the density of transmitters decreases, and hence the accuracy falls. For $r_{IBM} = 40, 60$ and $120$, higher values of the interference range compensate for the decrement of the accuracy index.

For ultra sparse networks, accuracy is determined by the probability of false alarm only. In IBM $P_{fa} = 0$, hence from Equation (3) IAC approaches unity because in sparse networks probability of miss-detection is negligible. Therefore higher values of accuracy are obtained for an average inter-transmitter distance of more than 160 m. Moreover, for ultra-dense networks modeled with IBM and inter-transmitter distances ranging between 0 m to 20 m, IAC depends on the probability of miss-detection only. As the average inter-transmitter distance decreases $P_{md}$ also decreases and IAC approaches unity.

The dip in a curve for $r_{IBM} = 20$ is because of the minimum value of interference range chosen which includes the minimum number of active transmitters, at the same time with minimum inter-transmitter distance and hence the high probability of miss-detection. This results in a significant reduction of IAC. From Figure 3 it is evident that with a high transmitter density at $d_t = 80$ m, and the same interference range, $P_{md}^{PRM} < P_{md}^{IBM}$. This improves the performance of IBM in the detection of outage events with the least error and high accuracy as shown in Figure 2. For the same network setting, $P_{fa}$ is not displayed in the graph for the sake of clarity. For large inter-transmitter distances, the network becomes very sparse. In this scenario $\xi = 1$, hence IAC is determined by $P_{fa}$ only.

For the same network conditions, we have calculated the KL divergence and Bhattacharyya distance for $r_{IBM} = 20, 60$. Figure 4 shows the plot of the Accuracy index with respect to an inter-transmitter distance. As already discussed lower values of KL and BC distance indicate higher accuracy of two probability distributions. Figure 4 illustrates that two distributions converge when the network is dense and the inter-transmitter distance is less. With an increase in inter-transmitter distance, the density of the network decreases, and two graphs fail to converge with $r_{IBM} = 20$. Therefore, the accuracy of these classical distance measures holds for lower inter-transmitter distance. Instead, an IAC takes into account a single threshold value for the comparison of distributions. Hence IAC proves to be a better distance measuring index as it gives a proper insight into the distance between $f_{\Upsilon^{IBM}}$ and $f_{\Upsilon^{PhyM}}$.

### A. Proposed Work

**Case II / Scenario-II:** Evaluation of the accuracy of reference interference models with respect to the test model.
**Type of communication:** Directional/mmWave
**Type of channel:** Deterministic
Assumptions for use of simplified interference model:
The simplified interference model with the assumptions explained below is used to study the impact of directionality and blockage on the performance of interference models in the estimation of IAC. Consider a homogenous Poisson network as assumed in scenario 1. To study the accuracy of interference models in mmWave networks, directional communication is taken into an account. This results in the suppression of interference in a wireless network.mmWaves undergo minimum scattering [31], hence the resulting narrow beam makes the channel more deterministic in contrast to the microwave systems[32].

The link between the transmitter i and the receiver located at the origin of Figure 1 is said to be in LOS with probability $e^{-\epsilon\lambda_0 d_{ij}}$ ($\epsilon$ is the size of an obstacle and $\lambda_0$ gives the density of obstacles) if there is an obstacle in between [33]. To rule out the beam searching phase[34] it is assumed that each transmitter and its intended receiver are properly aligned. The antenna pattern used at both UT and BSs is modeled by an Ideal sector model [30]. In this model, an antenna gain is considered to be constant in the main lobe and is expressed by $2\pi - (2\pi - \theta)z$. Here $z$ is a constant smaller antenna gain of the side lobe, $0 \leq z < 1$. For mathematical tractability operating beamwidth $\theta$ of UT and BSs is considered to be the same in both transmitting and receiving modes.
Interference can occur in a network in the following three cases:

1) If the receiver is inside the main lobe of an intended transmitter. The probability of occurrence of such an event is $\theta/2\pi$.

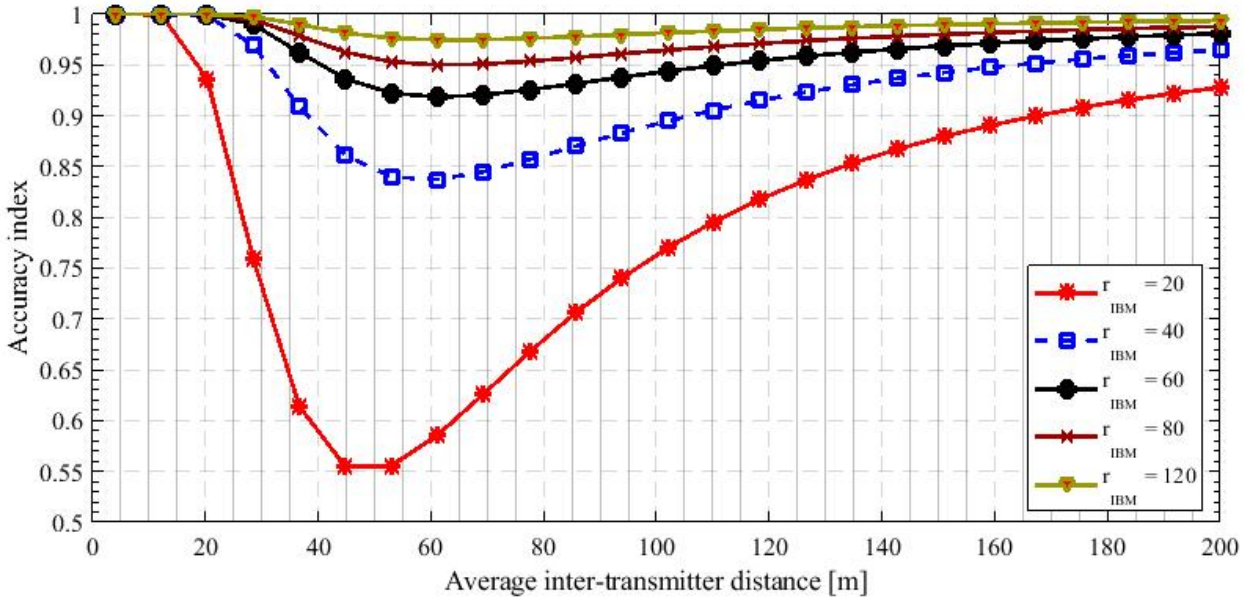


Figure 2. Impact of transmitter density on the accuracy of the IBM under Rayleigh fading channel.

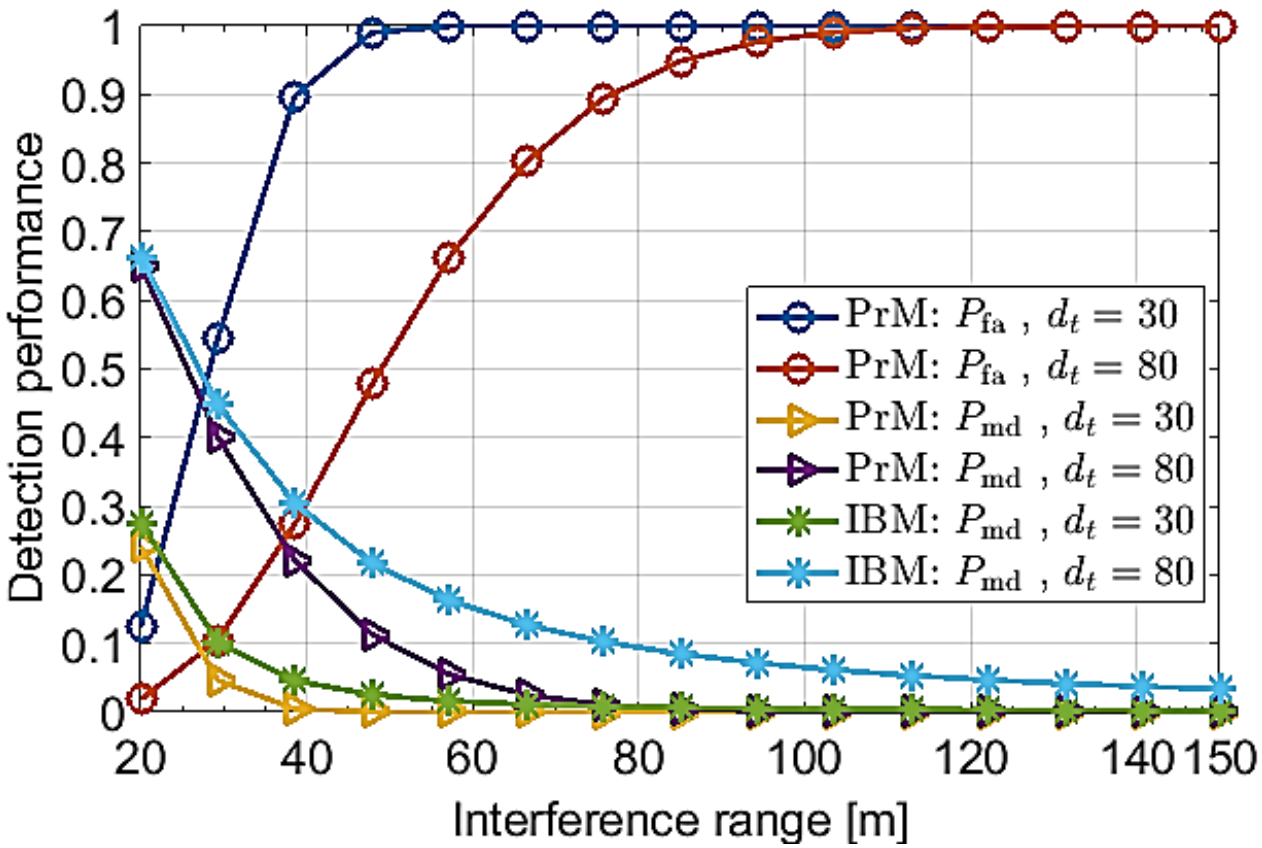


Figure 3. Error probabilities and Impact of the interference range on the accuracy of interference models under the Rayleigh fading channel

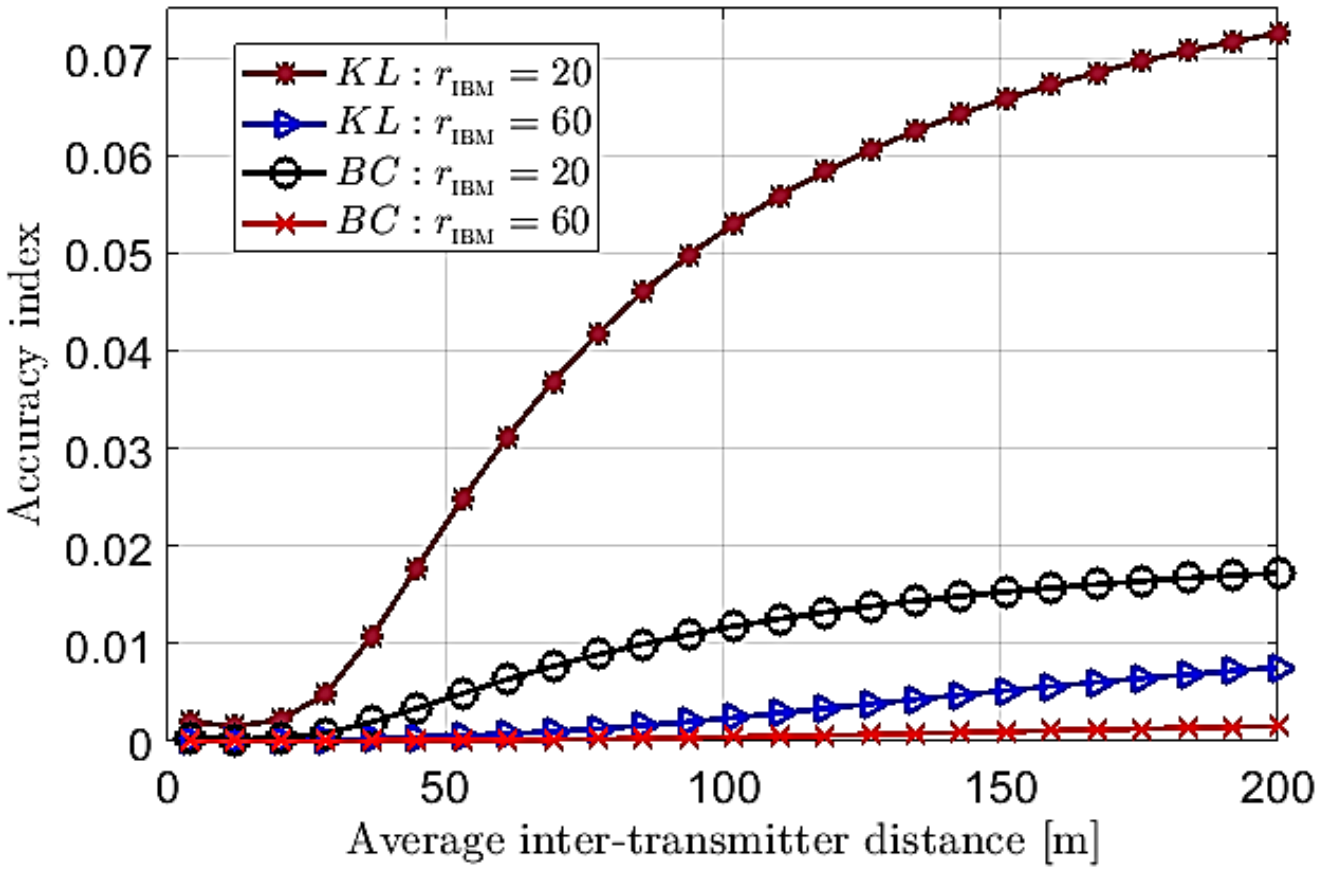


Figure 4. The KL divergence and Bhattacharyya distance of distribution from corresponding to the IAC values of Figure 2

2) If the intended transmitter is inside the main lobe of a receiver.
3) If the intended transmitter and receiver are in LOS.

The number of transmitters and a receiver share independent LOS links in a network. This implies that for cases 1 and 3 interferers are governed by the inhomogeneous point process represented by $\lambda_I$.

$\therefore$ At a radial distance $r$

$$\lambda_I(r) = \frac{\lambda_t \theta e^{-\epsilon\lambda_0 r}}{2\pi}$$

Consider case 2 where r takes any minimum value $R$ and therefore confines interferers to an annular region $A(\theta, 0, R)$ as shown in Figure 1. The average number of interferers inside this region is given by [35] as:

$$\begin{aligned} N_{A(\theta,0,R)} &= \theta \int_0^R \lambda_I(r) r dr \\ &= \frac{\theta^2 \lambda_t}{2\pi\epsilon^2\lambda_0^2}\left(1 - (1 + \epsilon\lambda_0 R)\, e^{-\epsilon\lambda_0 R}\right) \end{aligned} \tag{19}$$

To investigate the effect of directionality, we assume the product of the size and density of an obstacle approaching zero.

$\Rightarrow \epsilon\lambda_0 \to 0$
Applying the series expansion of $e^x$, we get

$$\begin{aligned} \therefore N_{A(\theta,0,R)} &= \frac{\theta^2 \lambda_t R^2}{4\pi} \\ &= \left(\frac{\theta\lambda_t}{2\pi}\right)\left(\frac{\theta R^2}{2}\right) \end{aligned}$$

First-term gives the density of obstacle per unit area and the second term gives an area of an angular region. From this equation, it is evident that the number of potential interferers within an interference range depends on operating beamwidth $\theta$. Hence by virtue of narrow beams, the number of potential interferers decreases considerably. However, $N_{A(\theta,0,R)}$ can be infinite if the interference range $R$ approaches infinity, i.e., if, $R \to \infty$. Substituting in Equation (19), it converges to
$N_{A(\theta,0,r)} = \frac{\theta^2 \lambda_t}{2\pi\epsilon^2\lambda_0^2} < \infty$ if $\epsilon\lambda_0 > 0$
$\epsilon\lambda_0 > 0$ infers that for a considerable blockage, there exists a finite number of interferers at the receiver end.

For mmWaves, the wavelength is smaller as compared to microwaves which implies high penetration loss and severe attenuation. This results in significant attenuation of a signal because most of the objects present in the network

contribute to blockage owing to their size and density. Thus the contribution of interference by transmitters located away from a typical receiver is diminished by directionality and blockage. The major contribution to interference is from the transmitters located closer to a typical receiver. In such a scenario these finite numbers of interferers can also cause a significant contribution to an aggregated interference term if placed close to a receiver.

As already explained in scenario 1, $P_{fa}^{IBM/PhyM} = 0$, hence the probability of miss-detection can be calculated by introducing $\theta/2\pi$ in equations (9) and (18) we get the following Equations [35]:

$$P_r\left[\gamma^{IBM} < \beta\right] = 1 - \exp\left\{\left(\frac{-n\theta^2\beta d_0^\alpha}{4\pi^2\times p\times c}\right) - \frac{\theta^2}{2\pi}\lambda_t E_h \left[\left(1 - e^{-\beta d_0^\alpha h}\right)\left(\frac{1-(\epsilon\lambda_0 a+1)e^{-\epsilon\lambda_0 a}}{\epsilon^2\lambda_0^2}\right) + \int_a^{r_{IBM}}\left(1 - e^{-\beta d_0^\alpha h r^{-\alpha}}\right)e^{-\epsilon\lambda_0 r} r dr\right]\right\} \quad (20)$$

and

$$P_r\left[\gamma^{PhyM} < \beta\right] = 1 - \exp\left\{\left(\frac{-n\theta^2\beta d_0^\alpha}{4\pi^2\times p\times c}\right) - \frac{\theta^2}{2\pi\epsilon^2\lambda_0^2}\lambda_t E_h \left[1 - e^{-\beta d_0^\alpha h}\left(1 - (1 + a\epsilon\lambda_0)\, e^{-a\epsilon\lambda_0}\right) - \epsilon^2\lambda_0^2\int_a^\infty\left(e^{-\beta d_0^\alpha h r^{-\alpha} - \epsilon\lambda_0 r}\right) r dr\right]\right\} \quad (21)$$

For numerical solutions, we can substitute the above equations in Equation 17 to obtain an expression for $P_{md}^{IBM/PhyM}$. To quantify IAC substitute values of Pmd and Pfa in Equation 3. As the interference range in IBM approaches infinity, IAC tends to unity, i.e two interference models become similar in detecting outage events. Simulation results of this scenario are obtained with the assumptions given in Table I of [5]. Here the study of variations in IAC of IBM and PRM due to operating beamwidth and average inter-transmitter distance is done. From Figure 5, it is indicated that at operating beamwidth $\theta = 20°$ for both IBM and PRM accuracy is improved due to directionality of signal and blockage by obstacles in mmWave communication.

Now by replacing the Rayleigh channel with the deterministic wireless channel as is a case in mmWave networks, it is observed that the accuracy of interference models IBM and PRM is further improved both at $\theta = 20°$ and $\theta = 40°$. From Figure 6 it is deduced that PRM can be used instead of IBM with accuracy index IAC = 1 in detecting outage events. If beamwidth is further reduced to pencil beams e.g., the accuracy of PRM for detecting outage events will approach unity. Hence in such network settings, it will be preferable to use PRM over IBM and PhyM due to its mathematical tractability.

The above results give a qualitative overview of interference models used in mmWave networks. This allows the use of simpler and more accurate interference models. The simpler and more accurate model thus proposed for mmWave networks is the simplification of PRM in which we consider impenetrable obstacles i.e., high penetration loss and zero sidelobe gain.

It is shown that despite the above-mentioned assumptions, the simplified interference model is still able to detect outage events accurately in mmWave networks. [12], [36] has used PRM for the development of protocols in a mmWave cellular network. Our work compliments such previous studies.

The accuracy of the interference model in this work is estimated using IAC. This quantifies the similarity of two distributions at a specific threshold instead of an entire range of SINR values. Later cases lead to misleading results where one can use a marginally accurate but complex interference model. In this work, it is proven that for mmWave cellular networks tractable and more accurate interference models can be used to investigate the performance of a network.

On the other hand, in this work, the assumption of equal transmission power at all nodes is taken into account. In more realistic cases, this assumption will not always hold true. Taking into consideration the realistic assumptions, the interference modeling will become complex.

Furthermore, IAC is used to access the accuracy of the two-ball blockage model. According to this model if BSs follow a homogenous Poisson point process (PPP) then the links connecting BS and UE are modeled under three events. The three states of links are statistically defined as:

1) 1. If there is no blockage between UE and BS then a link is under the LOS event.
2) If the link between BS and UE is blocked by obstacles, then a link is in an NLOS event.
3) If path loss between UE and BS approaches infinity then no link is established in a network.

This approach of the three-state link statistical model has not been adopted much for use in mmWave networks as reported in the literature [30]. The striking feature of this model is a non-zero probability of occurrence of an outage event. This is explored advantageously for ultra-dense networks where BSs in outage cannot contribute to an aggregated interference term as proved in the following section. The following points are observed in the 2-ball blockage model approximations for mmWave networks.

1) 1. If the average size of a cell ($D_1$) is 50 m with zero probability of occurrence of an outage event then the probability of an encompassing UE being connected through the LOS link is greater than 80%[5], [37]. In other words, if the distance from BS to UE is $r < D_1$, then the link can either be in LOS or NLOS state but the probability of being in LOS > 80%.In this case, mmWave cellular systems perform better than microwaves by providing improved coverage and better data rates.
2) If $50m < r < 200m(D_2)$, a link can be in LOS, NLOS or outage state. Most probably UE will be served by NLOS BS.
3) If $r > 200m(D_2)$, the communication link between

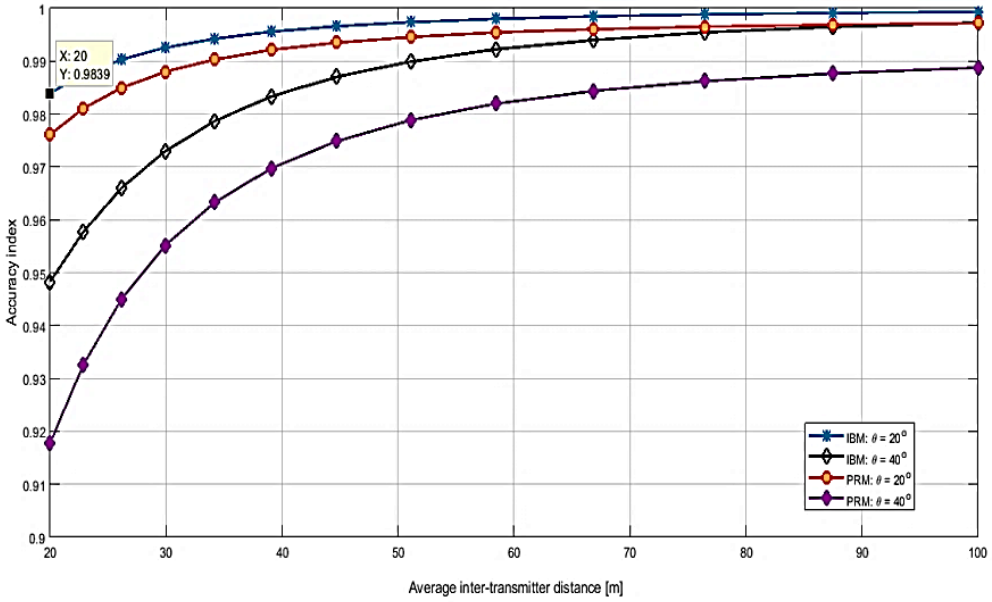


Figure 5. Accuracy of IBM and PRM under Rayleigh fading channel and directional communications

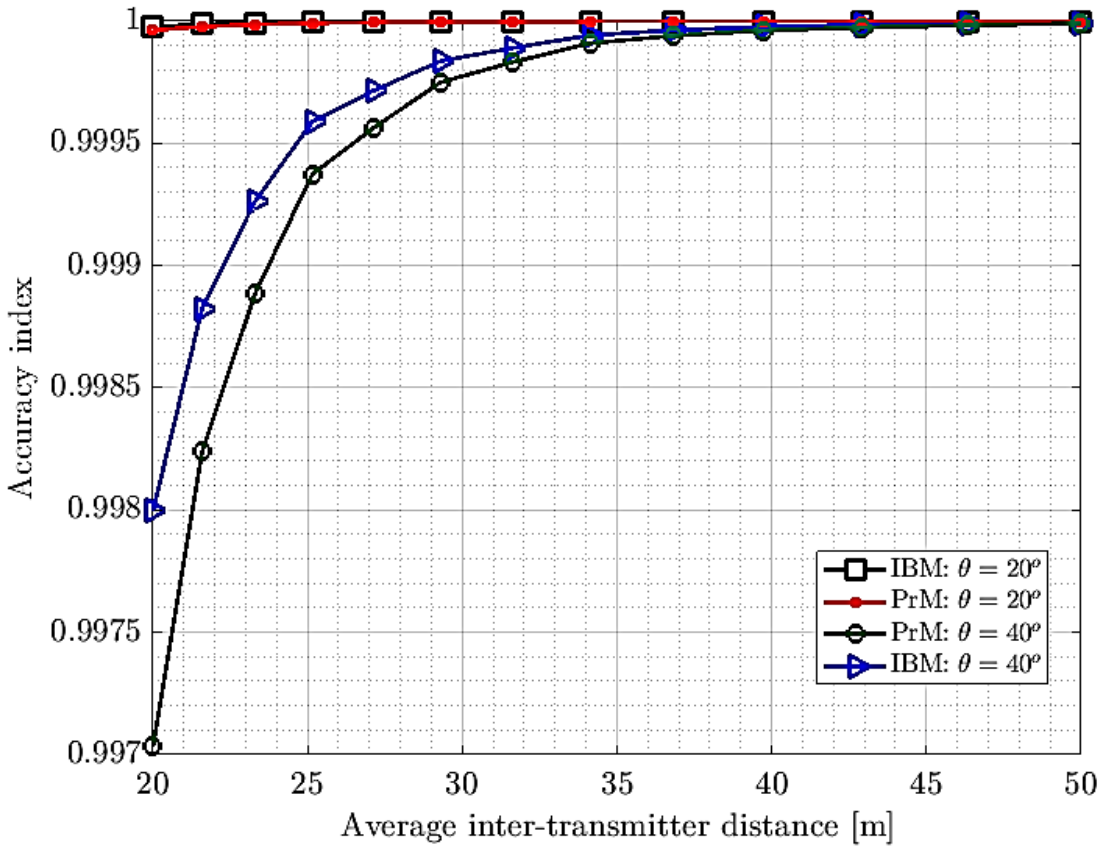


Figure 6. Accuracy of IBM and PRM under mmWave Communications and Deterministic channel

UE and BS will be in an outage.

4) $D_2$ signifies the upper limit of an operating range of mmWave communication that agrees with the conclusion of [5], [37].

An event where all the BSs will be in outage and UE cannot be connected to a network through any link occurs due to the presence of a blockage. If BSs are modeled as points of homogenous PPP then, the probability of occurrence of such event is defined by three independent link states as under.

$$\psi = \psi_{LOS} \cup \psi_{NLOS} \cup \psi_{OUT}$$

The third approximation of the two-ball model is concluded by considering

$$\psi_{LOS} = \psi_{NLOS} = \phi$$

$$\therefore \psi_{LOS} \cap \psi_{NLOS} = \phi$$

From definition $P_{LOS} + P_{NLOS} + P_{Blockage} = 1$

$$P_{LOS} + P_{NLOS} \leq 1$$

At minimum reliability threshold T, coverage probability is given by[38].

$$P^{\text{Cov}}(T) = P[SINR \geq T] = P[\gamma \geq T]$$

Thus for $T = 0$, the probability of coverage is zero. This will occur when $P_{LOS}(r) = 0$ and $P_{NLOS}(r) = 0$ and $P_{OUT}(r) = 1$. Hence the probability of blockage $P_{\text{blockage}} = 1$. As already discussed this corresponds to distance $D_2$ between UE and BS. Thus the two-ball approximation is considered to be a generalization of the single-ball model used in [32], [39]. In comparison with the study carried out in these papers, a two-ball model specifically takes into account the blockage owing to the outage state which is a characteristic feature of mmWave communications.

## 5. CONCLUSION

An analytical and numerical investigation of 5G mmWave networks is carried out for the design of a simpler interference model. IAC is used for the evaluation of the accuracy of existing interference models. It is observed that the accuracy of interference models is enhanced in mmWave networks with deterministic channels. The comparison of the Interference Ball Model (IBM) and Protocol Model (PRM) shows that accuracy is improved by considering infinite penetration loss and zero sidelobe antenna gain. This is a typical assumption for mmWave networks which further enhances the performance of PRM. The two-ball model is explored for use in mmWave networks and proves to supersede the existing ball model. IAC is further used to find the accuracy of the two-ball model and analyze the SINR distributions. Interference models for 5G mmWave networks can be developed for various other network scenarios where mobility of UEs can be taken into account for the evaluation of the trade-off between accuracy and tractability. Also, in this work, we assume that all transmitters have equal transmission power P. This work can be extended by assuming a more realistic case where each transmitter can transmit signals with different power. MATLAB is used for simulation and

## APPENDIX

Appendix A

$$\begin{aligned}
P_r\left[\gamma^{IBM} < \beta\right] &= P_r\left[\frac{h_0 \times d_0^{-\alpha}}{\sum_{k\in\mathfrak{T}\cap A(2\pi,0,r_{IBM})} h_k \times d_k^{-\alpha 1_{\bar{A}(2\pi,0,a)}} + \eta/p\times c} < \beta\right] \\
&= P_r\left[\frac{h_0}{\left(\sum_{k\in\mathfrak{T}\cap A(2\pi,0,r_{IBM})} h_k \times d_k^{-\alpha 1_{\bar{A}(2\pi,0,a)}} + \eta/p\times c\right) d_0^{\alpha}} < \beta\right] \\
&= P_r\left[h_0 < \left(\sum_{k\in\mathfrak{T}\cap A(2\pi,0,r_{IBM})} h_k \times d_k^{-\alpha 1_{\bar{A}(2\pi,0,a)}} + \eta/p\times c\right)\beta d_0^{\alpha}\right] \\
&= 1 - E_{I,h}\left[\exp\left\{-\left(\sum_{k\in\mathfrak{T}\cap A(2\pi,0,r_{IBM})} h_k \times d_k^{-\alpha 1_{\bar{A}(2\pi,0,a)}} + \eta/p\times c\right)\beta d_0^{\alpha}\right\}\right] \\
&= 1 - \exp\left(\frac{-\eta\beta d_0^{\alpha}}{p\times c}\right) E_{I,h}\left[\exp\left\{-\left(\sum_{k\in\mathfrak{T}\cap A(2\pi,0,r_{IBM})} h_k \times d_k^{-\alpha 1_{\bar{A}(2\pi,0,a)}}\right)\beta d_0^{\alpha}\right\}\right]
\end{aligned}$$

Appendix B

Using integration by parts,

$$\begin{aligned}
G(\xi) &= \exp\left\{-2\pi\lambda_t E_h\left[\int_0^a r dr - \int_o^a \left(e^{-\beta d_0^r h}\right) r dr + \int_a^{r_{IBM}} \left(1 - e^{-\beta d_0^{\alpha} h r^{-\alpha}}\right) r dr\right]\right\} \\
&= \exp\left\{-2\pi\lambda_t E_h\left[\frac{a^2}{2}\left(1 - e^{-\beta d_0^{\alpha} h}\right) + \int_a^{r_{IBM}} \left(1 - e^{-\beta d_0^{\alpha} h r^{-\alpha}}\right) r dr\right]\right\}
\end{aligned}$$

Solving second integral $\int_a^{r_{IBM}} \left(1 - e^{-\beta d_0^{\alpha} h r^{-\alpha}}\right) r dr$
put $\beta d_0^{\alpha} h = k$, $r = x$, $\alpha = a$, $a = b$, $r_{IBM} = c$

$$\int_a^{r_{IBM}} \left(1 - e^{-\beta d_0^{\alpha} h r^{-\alpha}}\right) r dr = \int_b^c \left(1 - e^{k x^{-a}}\right) x dx$$

By using a special integral for the incomplete gamma function and performing some mathematical manipulations, we get

$$\begin{aligned}
\int_b^c \left(1 - e^{k x^{-a}}\right) x dx &= \frac{(c-b)(c+b)}{2} - \frac{\Gamma\left(\frac{2}{a}, \frac{k}{c^a}\right) - \Gamma\left(-\frac{2}{a}, \frac{k}{b^a}\right)}{a} k^{\frac{2}{a}} \\
&= \frac{(c^2 - b^2)}{2} - \left[\frac{\Gamma\left(\frac{2}{a}, \frac{k}{c^a}\right) - \Gamma\left(-\frac{2}{a}, \frac{k}{b^a}\right)}{a}\right] k^{\frac{2}{a}}
\end{aligned}$$

Substituting back the values, we have

$$= \frac{(r_{IBM}^2 - a^2)}{2} - \left[\Gamma\left(\frac{2}{\alpha}, \frac{\beta d_0^{\alpha} h}{r_{IBM}^{\alpha}}\right) - \Gamma\left(-\frac{2}{\alpha}, \frac{\beta d_0^{\alpha} h}{a^{\alpha}}\right)\right] \frac{(\beta d_0^{\alpha} h)^{2/\alpha}}{\alpha}$$

$$G(\xi) = \exp\left\{-2\pi\lambda_t E_h\left[\frac{a^2}{2}\left(1 - e^{-\beta d_0^{\alpha} h}\right) + \left(\frac{r_{IBM}^2 - a^2}{2}\right) - \left[\Gamma\left(\frac{2}{\alpha}, \frac{\beta d_0^{\alpha} h}{r_{IBM}^{\alpha}}\right) - \Gamma\left(-\frac{2}{\alpha}, \frac{\beta d_0^{\alpha} h}{a^{\alpha}}\right)\right] \frac{(\beta d_0^{\alpha} h)^{2/\alpha}}{\alpha}\right]\right\}$$

Put the above value in Equation (8), Equation (9) is obtained.

From Bayes' theorem,

$$P[A/B] = \frac{P(A).P(B/A)}{P(B)} = \frac{P(A).P(B/A)}{1 - P(A)}$$

## References


[1] M. Attaran, "The impact of 5g on the evolution of intelligent automation and industry digitization," *Journal of Ambient Intelligence and Humanized Computing*, pp. 1–17, February 2021.

[2] S. Niknam, R. Barazideh, and B. Natarajan, "Cross-layer interference modeling for 5g mmwave networks in the presence of blockage," in *2018 IEEE 88th Vehicular Technology Conference (VTC-Fall)*. IEEE, August 2018, pp. 1–5.

[3] S. Rangan, T. S. Rappaport, and E. Erkip, "Millimeter-wave cellular wireless networks: Potentials and challenges," *Proceedings of the IEEE*, vol. 102, no. 3, pp. 366–385, March 2014.

[4] H. Shokri-Ghadikolaei, C. Fischione, G. Fodor, P. Popovski, and M. Zorzi, "Millimeter wave cellular networks: A mac layer perspective," *IEEE Transactions on Communications*, vol. 63, no. 10, pp. 3437–3458, October 2015.

[5] M. R. Akdeniz, Y. Liu, M. K. Samimi, S. Sun, S. Rangan, T. S. Rappaport, and E. Erkip, "Millimeter wave channel modeling and cellular capacity evaluation," *IEEE journal on selected areas in communications*, vol. 32, no. 6, pp. 1164–1179, June 2014.

[6] U. Ali, G. Caso, L. De Nardis, K. Kousias, M. Rajiullah, Ö. Alay, M. Neri, A. Brunstrom, and M.-G. Di Benedetto, "Large-scale dataset for the analysis of outdoor-to-indoor propagation for 5g midband operational networks," *Data*, vol. 7, no. 3, p. 34, march 2022.

[7] A. Ephremides, J. E. Wieselthier, and D. J. Baker, "A design concept for reliable mobile radio networks with frequency hopping signaling," *Proceedings of the IEEE*, vol. 75, no. 1, pp. 56–73, 1987.

[8] A. Iyer, C. Rosenberg, and A. Karnik, "What is the right model for wireless channel interference?" *IEEE Transactions on Wireless Communications*, vol. 8, no. 5, pp. 2662–2671, May 2009.

[9] T. S. Rappaport, R. W. J. Heath, R. C. Daniels, and J. Murdock, *Millimeter Wave Wireless Communications*. Upper Saddle River, NJ,USA: Prentice-Hall, 2015.

[10] P. Gupta and P. R. Kumar, "The capacity of wireless networks," *IEEE Transactions on information theory*, vol. 46, no. 2, pp. 388–404, March 2000.

[11] K. Xu, M. Gerla, and S. Bae, "How effective is the ieee 802.11 rts/cts handshake in ad hoc networks," in *IEEE Global Telecommunications Conference(GLOBECOM)*, vol. 1. IEEE, 2002, pp. 72–76.

[12] S. Singh, R. Mudumbai, and U. Madhow, "Interference analysis for highly directional 60-ghz mesh networks: The case for rethinking medium access control," *IEEE/ACM Transactions on networking*, vol. 19, no. 5, pp. 1513–1527, October 2011.

[13] Y. Xu, H. Shokri-Ghadikolaei, and C. Fischione, "Distributed association and relaying with fairness in millimeter wave networks," *IEEE Transactions on Wireless Communications*, vol. 15, no. 12, pp. 7955–7970, December 2016.

[14] M. K. Marina, S. R. Das, and A. P. Subramanian, "A topology control approach for utilizing multiple channels in multi-radio wireless mesh networks," *Computer networks*, vol. 54, no. 2, pp. 241–256, February 2010.

[15] T. Stahlbuhk, B. Shrader, and E. Modiano, "Topology control for wireless networks with highly-directional antennas," in *IEEE International Symposium on Modeling and Optimization in Mobile, Ad Hoc, and Wireless Networks (WiOpt)*. IEEE, 2016, pp. 1–8.

[16] K. Jain, J. Padhye, V. N. Padmanabhan, and L. Qiu, "Impact of interference on multi-hop wireless network performance," *Wireless networks*, vol. 11, no. 4, pp. 471–487, 2005.

[17] A. E. Gamal, J. Mammen, B. Prabhakar, and D. Shah, "Throughput-delay trade-off in wireless networks," in *IEEE International Conference on Computer Communications (INFOCOM)*, vol. 1. IEEE, 2004, pp. 464–475.

[18] A. El Gamal, J. Mammen, B. Prabhakar, and D. Shah, "Optimal throughput–delay scaling in wireless networkspart ii: Constant-size packets," *IEEE Transactions on Information Theory*, vol. 52, no. 6, pp. 2568–2592, June 2006.

[19] G. D. Celik, G. Zussman, W. F. Khan, and E. Modiano, "Mac for networks with multipacket reception capability and spatially distributed nodes," *IEEE Transactions on Mobile Computing*, vol. 9, no. 2, pp. 226–240, August 2009.

[20] H. Shokri-Ghadikolaei, C. Fischione, and E. Modiano, "On the accuracy of interference models in wireless communications," in *2016 IEEE International Conference on Communications (ICC)*. IEEE, May 2016, pp. 1–6.

[21] L. B. Le, E. Modiano, C. Joo, and N. B. Shroff, "Longest-queue-first scheduling under sinr interference model," in *ACM International Symposium on Mobile Ad hoc Networking and Computing (MobiHoc)*, 2010, pp. 41–50.

[22] S. P. Weber, X. Yang, J. G. Andrews, and G. De Veciana, "Transmission capacity of wireless ad hoc networks with outage constraints," *IEEE transactions on information theory*, vol. 51, no. 12, pp. 4091–4102, December 2005.

[23] S. P. Weber, J. G. Andrews, X. Yang, and G. De Veciana, "Transmission capacity of wireless ad hoc networks with successive interference cancellation," *IEEE Transactions on Information Theory*, vol. 53, no. 8, pp. 2799–2814, August 2007.

[24] M. Di Renzo, "Stochastic geometry modeling and analysis of multi-tier millimeter wave cellular networks," *IEEE Transactions on Wireless Communications*, vol. 14, no. 9, pp. 5038–5057, September 2015.

[25] S. A. Jafar, "Topological interference management through index coding," *IEEE Transactions on Information Theory*, vol. 60, no. 1, pp. 529–568, January 2013.

[26] X. Yi and D. Gesbert, "Topological interference management with transmitter cooperation," *IEEE Transactions on Information Theory*, vol. 61, no. 11, pp. 6107–6130, November 2015.

[27] S. Kullback, "Solomon kullback, information theory and statistics," *The Mathematical Gazette*, vol. 54, no. 387, pp. 90–90, 1970.

[28] T. S. Rappaport, *Wireless communications: principles and practice*, 2nd ed. Upper Saddle River, NJ, USA: Prentice-Hall, 2002.

[29] A. Bobrowski, *Functional analysis for probability and stochastic processes: an introduction*. Cambridge University Press, 2005.

[30] M. Di Renzo, "Stochastic geometry modeling and analysis of multi-tier millimeter wave cellular networks," *IEEE transactions on Communications*, vol. 14, no. 9, pp. 5038–5057, September 2015.

[31] Y. Banday, G. Mohammad Rather, and G. R. Begh, "Effect of atmospheric absorption on millimetre wave frequencies for 5g cellular networks," *IET Communications*, vol. 13, no. 3, pp. 265–270, 2018. [Online]. Available: https://ietresearch.onlinelibrary.wiley.com/doi/abs/10.1049/iet-com.2018.5044

[32] T. S. Rappaport, G. R. MacCartney, M. K. Samimi, and S. Sun, "Wideband millimeter-wave propagation measurements and channel models for future wireless communication system design," *IEEE transactions on Communications*, vol. 63, no. 9, pp. 3029–3056, September 2015.

[33] T. Bai, R. Vaze, and R. W. Heath, "Analysis of blockage effects on urban cellular networks," *IEEE Transactions on Wireless Communications*, vol. 13, no. 9, pp. 5070–5083, September 2014.

[34] H. Shokri-Ghadikolaei, L. Gkatzikis, and C. Fischione, "Beam-searching and transmission scheduling in millimeter wave communications," in *IEEE International Conference on Communications (ICC)*. IEEE, 2015, pp. 1292–1297.

[35] H. Shokri-Ghadikolaei, C. Fischione, and E. Modiano, "Interference model similarity index and its applications to millimeter-wave networks," *IEEE Transactions on Wireless Communications*, vol. 17, no. 1, pp. 71–85, 2017.

[36] S. Singh, F. Ziliotto, U. Madhow, E. Belding, and M. Rodwell, "Blockage and directivity in 60 ghz wireless personal area networks: From cross-layer model to multihop mac design," *IEEE Journal on Selected Areas in Communications*, vol. 27, no. 8, pp. 1400–1413, October 2009.

[37] T. S. Rappaport, S. Sun, R. Mayzus, H. Zhao, Y. Azar, K. Wang, G. N. Wong, J. K. Schulz, M. Samimi, and F. Gutierrez, "Millimeter wave mobile communications for 5g cellular: It will work!" *IEEE access*, vol. 1, pp. 335–349, May 2013.

[38] M. Di Renzo and P. Guan, "Stochastic geometry modeling of coverage and rate of cellular networks using the gil-pelaez inversion theorem," *IEEE Communications Letters*, vol. 18, no. 9, pp. 1575–1578, September 2014.

[39] S. Singh, M. N. Kulkarni, A. Ghosh, and J. G. Andrews, "Tractable model for rate in self-backhauled millimeter wave cellular networks," *IEEE Journal on Selected Areas in Communications*, vol. 33, no. 10, pp. 2196–2211, 2015, to appear. [Online]. Available:http://arxiv.org/pdf/1407.5537v2.pdf.

**Yusra Banday** Yusra Banday earned her Ph.D. from Advance Communication Lab, at the National Institute of Technology, Srinagar Kashmir in 2021. She is a postdoctoral research scientist at the Indian Institute of Technology, Jammu, India. She has done M.Tech. in Communication Engineering. She received her Bachelors in Electronics & Communication Engineering from the University of Kashmir, India in 2011. She has also worked as a faculty in the National Institute of Technology, Srinagar, India. Her research interests include Millimeter Wave communication, RIS, High-speed Networks, and Next-generation Networks. Her research aims at understanding the interference phenomena in 5G networks and its management. Dr. Yusra is a student member of IEEE and IEEE MTTS society.

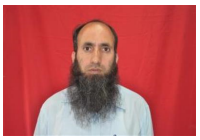

**Gh. Rasool Begh** Gh. Rasool Begh has received his Ph.D. from the National Institute of Technology Srinagar (J & K), India. He is working as an Associate Professor in the Department of Electronics and Communication Engineering at NIT Srinagar. He has teaching experience of more than 20 years. He has guided several scholars in the areas of OFDM, Cognitive Radios, WLANs, and Security. His areas of interest include Cognitive Radios, OFDM, MIMO, Cooperative Communications, Error control coding, RIS, Full Duplex communication and Security. Dr. Begh is is a member of the IEEE Communication Society.

**Ghulam Mohammad Rather** Ghulam Mohammad Rather, Ph.D. has done Ph.D. from IISC, Bangalore India in 1997. He is working as a Professor in the Department Of Electronics and Communication at NIT Srinagar. He received a B.E. degree in Electronics and Communications Engineering from the Kashmir University, India, in 1981, an M.S. degree (1988) in Computer Communications. He has teaching experience of more than 35 years. His research interests are in the field of Computer Networks, Millimeter Wave Communication, and the Internet of Things. Professor Rather is a member of IET and IEEE MTTS Society India.